Distinct Lobes of *Limulus* Ventral Photoreceptors

II. Structure and Ultrastructure

BRUCE G. CALMAN and STEVEN C. CHAMBERLAIN

From The Institute for Sensory Research, Syracuse University, Syracuse, New York 13210

ABSTRACT   The structure of *Limulus* ventral photoreceptors fixed in situ has been investigated using light and electron microscopy and computer-assisted reconstruction and planimetry. Photoreceptors occur singly and in clusters. All photoreceptors have two types of lobes. The rhabdomeral lobe (R lobe) appears to be specialized for light sensitivity, containing the rhabdomere, which completely covers its external surface and forms infoldings into the lobe. The structure of the external rhabdom differs from that within infoldings. The other main structures of the R lobe are the palisades along the rhabdom, multivesicular bodies, lamellar bodies, and mitochondria. The arhabdomeral lobe (A lobe) bears the axon and contains the nucleus, clusters of residual bodies, lamellar arrays of endoplasmic reticulum, masses of glycogen, lipid droplets, and Golgi complexes. The R lobe and A lobe are analogous to the outer and inner segments of vertebrate photoreceptors. In single photoreceptors A and R lobes are separated by an indentation filled with glial processes. Computer reconstructions of cell clusters reveal that each cell has both types of lobes and an axon. Most of the rhabdom is formed from abutting arrays of external rhabdom from the R lobes of different members of the cluster. Efferent fibers containing characteristic angular granules penetrate single cells and clusters in glial invaginations. The main, if not exclusive, target of the efferent fibers is the internal rhabdom.

INTRODUCTION

Since they were originally proposed for the physiological study of phototransduction (Millecchia et al., 1966), the ventral photoreceptors of *Limulus polyphemus* have become an important model system for studies of how photoreceptors transduce light. Among their advantages as a model system must be counted their large size, which allows multiple penetrations with intracellular electrodes and selective illumination of portions of the cell; the ease with which their extracellular environment can be manipulated; and their survival as transducing cells in vitro.

Despite their importance in physiological studies of phototransduction, the morphology of *Limulus* ventral photoreceptors has been relatively neglected. Before the advent of electron microscopy, there were a number of studies motivated by the suggestion made by Patten (1893) that during development, the ventral photoreceptors and ventral optic nerves metamorphosed into an olfactory structure in the adult. Subsequent studies (e.g., Patten, 1912; Hanström, 1926) established that these structures were visual, but it remained for the physiologists to conclusively demonstrate that the ventral photoreceptors were functioning visual organs (Millecchia et al., 1966; Millecchia and Mauro, 1969 a, b; Snodderly, 1971; Wasserman, 1973; Behrens and Fahey, 1981). Only one ultrastructural study and one abstract have been reported (Clark et al., 1969; Stell and Ravitz, 1970). It has been the operating assumption, based on the results of Clark et al., that the ventral photoreceptors contained rhabdom formed by invaginations of the cell membrane into the cytoplasm, and that the rhabdom was essentially randomly distributed within the ovoid of the photoreceptor soma. Recently, Bacigalupo et al. (1981) and Stern et al. (1982) have clearly demonstrated that ventral photoreceptors have functionally and structurally distinct segments or lobes. Here we report the results of a detailed light and electron microscope study of ventral photoreceptors fixed in vivo. Our results emphasize that each ventral photoreceptor has two distinct types of lobes: one that contains all the rhabdom and whose surface is covered with microvilli; and one that contains no rhabdom but much of the typical cytoplasmic machinery found in neurons of all sorts. The structure and ultrastructure of ventral photoreceptors is presented within the framework of this basic segmentation.

METHODS

Fixation and Embedding

Adult horseshoe crabs (*Limulus polyphemus*) measuring 20–25 cm across the carapace were used in this study. Animals were maintained in aquaria with circulated artificial seawater and regularly fed fresh clams. The light/dark cycle in ambient illumination was periodically adjusted to match local natural lighting. Animals were fixed in midmorning in normal room light by intracardial injection of a fixative containing 4.5% sucrose, 3% NaCl, 0.8% glutaraldehyde, and 5% formaldehyde in Sorensen's phosphate buffer at pH 7.2 (Fahrenbach, 1969). The ventral optic nerves remained in situ for 30 min after injection; then they were removed from the animal and immersed in fixative at 4°C overnight. They were then washed in 8% sucrose in phosphate buffer and postfixed in 1% OsO₄ in phosphate buffer for 1 h. Finally, they were washed in distilled water, dehydrated through an ethanol series to propylene oxide, and embedded in Epon-Araldite.

Light Microscopy

For observation with the light microscope, serial 1-μm sections were cut with a Sorvall MT2-B ultramicrotome (Dupont-Sorvall, Newtown, CT) using glass knives. Sections were mounted on glass slides and stained with 1% toluidine blue (Trump et al., 1961). Photomicrographs were prepared with a Nikon Biophot microscope (Nikon, Inc., Garden City, NY).

Electron Microscopy

Gold and silver thin sections were cut with glass knives on either a Sorvall MT2-B or a Sorvall MT5000 ultramicrotome and placed on naked copper grids. Sections were stained with uranyl acetate and lead citrate. Electron micrographs were prepared using a Siemens Elmiskop 101 electron microscope (Siemens Corp., Iselin, NJ).

Computer Reconstructions and Planimetry

Reconstructions of serially sectioned photoreceptors and photoreceptor clusters were made with the computer facilities of the Department of Anatomy at the SUNY Upstate Medical Center. Each 1-μm section in a serial set containing a cell or cell cluster was photographed with the light microscope. Then prints were used as maps on which to mark significant features while observing the section through the microscope. Structures to be digitized were traced on vellum and the alignment of adjacent sheets was determined by aligning the photomicrographs and transferring the alignment to the vellum sheets. The structures on each vellum sheet were then digitized on an acoustic tablet (Graf Pen, Science Accessories Corp., Southport, CT). After the x-y coordinates had been specified from the tablet and the z coordinate was entered for each section, the display software produced an image of the stacked serial set, viewed from an angle specified by the experimenter. Stereopairs[1] were then calculated, rotated, and displayed until an advantageous viewpoint was achieved. The stereopairs were plotted on a 7221A digital plotter (Hewlett-Packard, Inc., Palo Alto, CA). In the original plots each feature was shown in a different color.

The volumes of rhabdom were estimated from the vellum sheets. The area of each profile of each type of rhabdom was measured using planimetry software and the digitizing tablet. The volumes were then calculated by assuming that the profile in each 1-μm section was 1 μm thick.

RESULTS

Gross Anatomy of the Ventral Eye

The ventral eye of *Limulus* consists of the fused end organ, which overlies a portion of ventral cuticle just anterior to the mouth, and the bilateral ventral optic nerves, which connect the end organ to the brain (Fig. 1). The nerve trunks are encased in arterial sheaths that are continuous with the vascular sheath covering the protocerebrum and the rest of the central nervous system. The nerve trunks and end organ appear to contain only photoreceptor cell bodies, their afferent axons, glial cells, and efferent fibers from the protocerebrum that innervate the photoreceptors. The afferent axons enter the anterior surface of the protocerebrum ventrally, then turn dorsally before ultimately coursing posteriorly to the anteromedial surface of the medulla (Chamberlain, 1978; Batra et al., 1979). If the arterial sheath is removed, photoreceptor

---

[1] Stereopairs can be viewed with a standard viewer or by parallel eye inspection with the following technique. Hold a pencil at arm's length and look past it at distant objects. Notice the two images of the pencil. If a stereopair is substituted for the pencil, one will see four images. Seeing a stereopair in three dimensions involves making the two center images overlap exactly. It will then appear as a three-dimensional image with a flat image on either side. Rocking the stereopair from side to side may help one fuse the two central images.

somata are visible in living preparations scattered along the periphery of the nerve trunk. The observation of freshly dissected tissue can be enhanced by vitally staining the somata with neutral red (Battelle et al., 1979), which stains the residual bodies in the photoreceptor cytoplasm.[2] When viewed with the dissecting microscope, the somata appear as ovoid bodies of various sizes. There is great variability from nerve to nerve in the arrangement of photoreceptors along the length of the trunk. Generally, there are concentrations of somata in the end organ and sometimes near the photocerebrum.
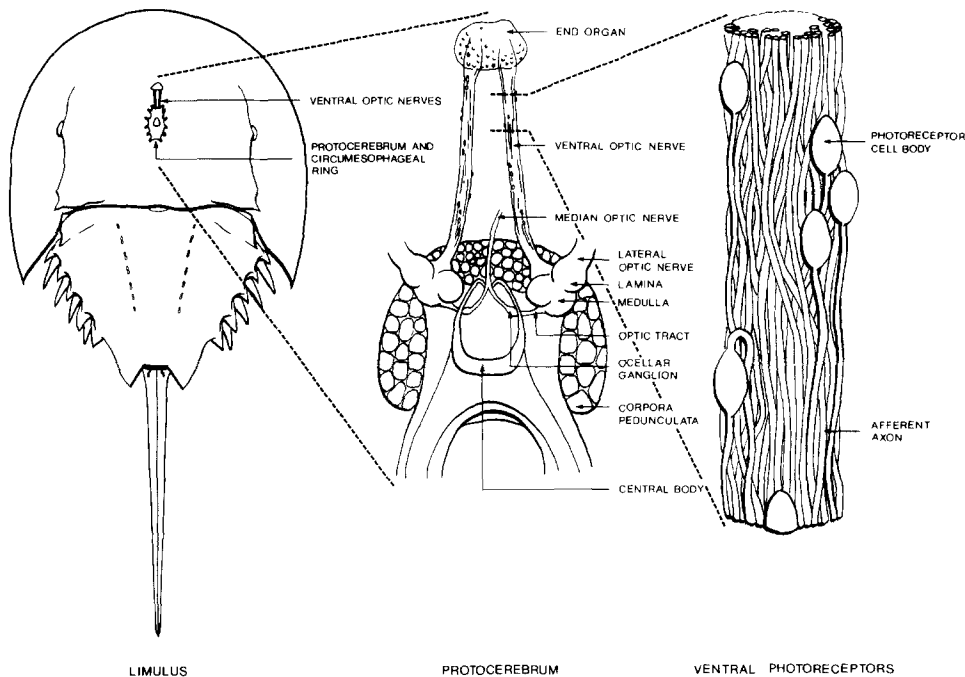

FIGURE 1.   Summary drawing of the anatomy of the *Limulus* protocerebrum and ventral optic nerves (see text for details).

Light Microscopy of Ventral Photoreceptors

When the ovoids observed with the dissecting microscope are fixed, sectioned, and observed with the light microscope, they are found to be sheathed in glia and to contain from one to six or more photoreceptor somata. The differential distribution of single cells and clusters of cells is variable.

Fig. 2 shows photomicrographs of single ventral photoreceptors. Longitudinal sections of single cells reveal a structural specialization of the cytoplasm into two types of regions. Adjacent regions are nearly always separated by a

[2] S. C. Chamberlain, B. A. Battelle, and B. G. Calman. Subcellular localization of neutral red staining in *Limulus* ventral photoreceptors. Manuscript in preparation.

glia-filled indentation along the surface of the cell; therefore we shall refer to them as lobes. One type of lobe, the rhabdomeral lobe (R lobe), usually occupies the end of the soma opposite the axon and contains the microvillous rhabdomere. The surface of the R lobe is completely covered with rhabdom, with occasional invaginations of rhabdom from the surface toward the interior of the R lobe. The cytoplasm of the R lobe stains lightly in plastic sections and is relatively uniform in appearance, sometimes appearing striated normal to the surface of the lobe. The other lobe, the arhabdomeral lobe (A lobe), contains no rhabdom, but possesses the cell nucleus, lipid droplets, and residual bodies, and gives rise to the axon. The cytoplasm is mottled with clumps of residual bodies and lipid droplets. Fig. 2A shows a longitudinal section near the center of a typical single photoreceptor having its R lobe and axon at opposite ends of the cell. Sometimes, however, the R lobe lies to the side of the cell (Fig. 2B) and, more rarely, one cell may have two R lobes (Fig. 2D). Some cells are relatively tiny, but still show the segmentation into R and A lobes (Fig. 2C). Such cells are 10–20 times smaller in volume than typical cells.

Clusters of cells have a different appearance in section (Fig. 3). One's first impression is that the rhabdom is internal to the cell; however, counting the nuclei in serial sections will yield the number of cells, and close inspection of the appearance of the cytoplasm reveals that most of the rhabdom is on the external surface of an R lobe. Thus the rhabdom in clusters lies on the external surface of the R lobes of the individual cells, but is buried within the mass of the cluster as it abuts the rhabdom from an adjacent cell. Although the apposition of rhabdomeres between cells is not nearly as well matched as it is between the retinular cells of the lateral compound eye, most of the rhabdom in clusters lies internally between abutting R lobes, with much less lying internally between an R lobe and an A lobe, and relatively little lying on the surface of the cluster as nonabutting external rhabdom of an individual R lobe. Each photoreceptor in a cluster contributes to the rhabdom, and each has a separate nucleus and axon.

The other rudimentary photoreceptors of *Limulus*, the lateral rudimentary eye and the endoparietal eye, have been observed with the light microscope. These photoreceptors show segmentation similar to that of ventral photoreceptors; however, it appears to be more common in these cells to have an R lobe abutting the A lobe of another cell.

Computer Reconstruction of Single and Clustered Photoreceptors

The light micrographs of Figs. 2 and 3 show sections from serial sets that were used to make the three-dimensional reconstructions shown in Figs. 4–7. In these stereopair reconstructions, the arrows mark the division between the R and A lobes in single cells and places where the rhabdom reaches the surface in clusters. The reconstructions shown are the bottom half of each cell viewed from above. In the A lobe, the lines represent the surface of the cell; in the R lobe, only rhabdom has been digitized. The reconstructions show that indeed,
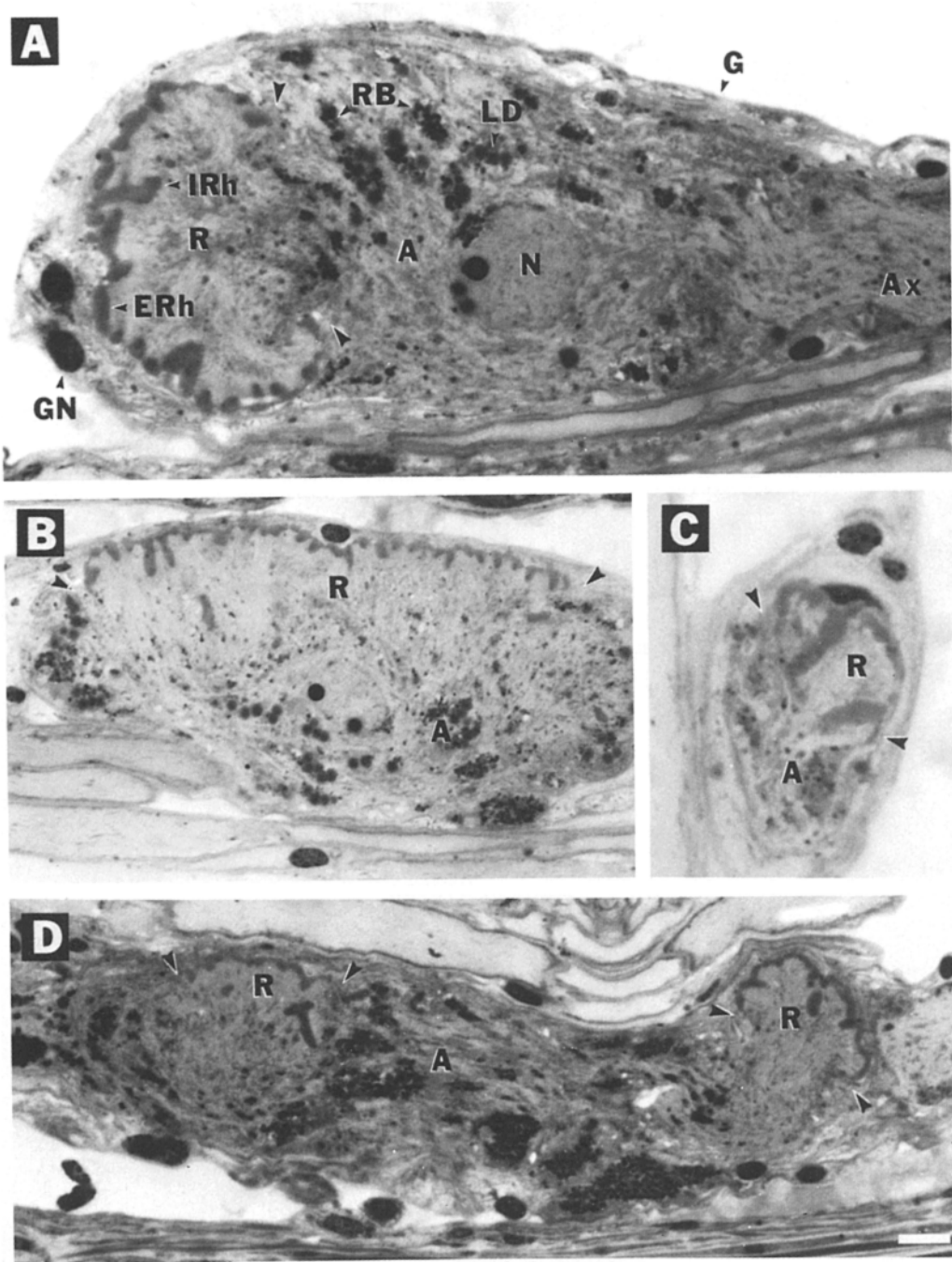
at this magnification, the entire surface of the R lobe is covered by rhabdom, and that the internal rhabdom in the R lobe is always continuous with external rhabdom on the surface. The rhabdomere of an R lobe in a single ventral photoreceptor is a continuous sheet curved to cover the surface of the R lobe with creases forming the internal rhabdom.

Computer-assisted planimetry was used to determine the volumes of the rhabdomeres, R lobes, and somata for the photoreceptors of Fig. 2. The results summarized in Table I show that most of the rhabdom volume (74–84%) occurs as external rhabdom. The rhabdom occupies a relatively constant percentage of the photoreceptor volume (3.5–6.4%) in a sample whose largest cell has 20 times the volume of the smallest cell.

Figs. 6 and 7 show the top and bottom halves of a computer reconstruction of a four-cell cluster. The rhabdom in clusters forms a single continuous structure lying mainly between cells with occasional invaginations into individual cells. Where the rhabdom reaches the surface of the cluster it may continue for a short distance along the surface of a single photoreceptor. We thus divided the rhabdom volume into three categories for computer-assisted planimetry; fused rhabdom external to individual R lobes but internal to the cluster; unfused external rhabdom lying on the surface of the cluster; and internal rhabdom within an individual cell. The results of volume measurements shown in Table II show that there is relatively less internal rhabdom in photoreceptors in clusters than in single photoreceptors. There may be relatively less rhabdom for the same total volume in clusters than in single cells, although our sample needs to be larger to confirm the trend of the data.

Tables I and II also give the estimated surface area of rhabdom per cell. The surface area was calculated from the estimates of rhabdom volume by modeling the rhabdom as an array of hexagonally close-packed, uniform cylinders. This model dictates that 9.3% of the measured rhabdom volume be considered extracellular space, which is probably a maximum estimate of the actual value. The average value of microvillar diameter we measured was 0.05 μm. With these assumptions, 1 μm^3 of measured rhabdom volume is equivalent to a surface area of 41 μm^2. The estimated surface areas range from 1.86 $\times$ 10^{-4} cm^2 for the smallest cell to 2.52 $\times$ 10^{-3} cm^2 for a large single cell. This is

FIGURE 2. (*opposite*) Photomicrographs of single ventral photoreceptors in *Limulus*. A. Longitudinal section of a single ventral photoreceptor bearing a rhabdomeral lobe on the left (R) and giving rise to an axon (Ax) on the right from the arhabdomeral lobe (A) in the center. This is the most common configuration of the segments of single photoreceptors. B. The R lobe lies on the side of the photoreceptor. C. The arrangement of the lobes is similar to A, but the cell is 16 times smaller in volume. D. The photoreceptor has two separate R lobes. Reconstruction of cells A and B are shown in Figs. 4 and 5. The pairs of arrows indicate the junctions of the R lobe and A lobe at the external surface. A: arhabdomeral lobe; Ax: axon; ERh: external rhabdom; G: glial cells; GN: glial cell nucleus; IRh: internal rhabdom; LD: lipid droplet; N: photoreceptor nucleus; R: rhabdomeral lobe; RB: residual bodies. The bar in D represents 7.5 μm in A, 11 μm in B, 6.3 μm in C, and 11.6 μm in D.

comparable to the estimate of 4×10^{-3} cm^2 for the average surface area of the ventral photoreceptor from membrane capacitance measurements (Fain and Lisman, 1981).
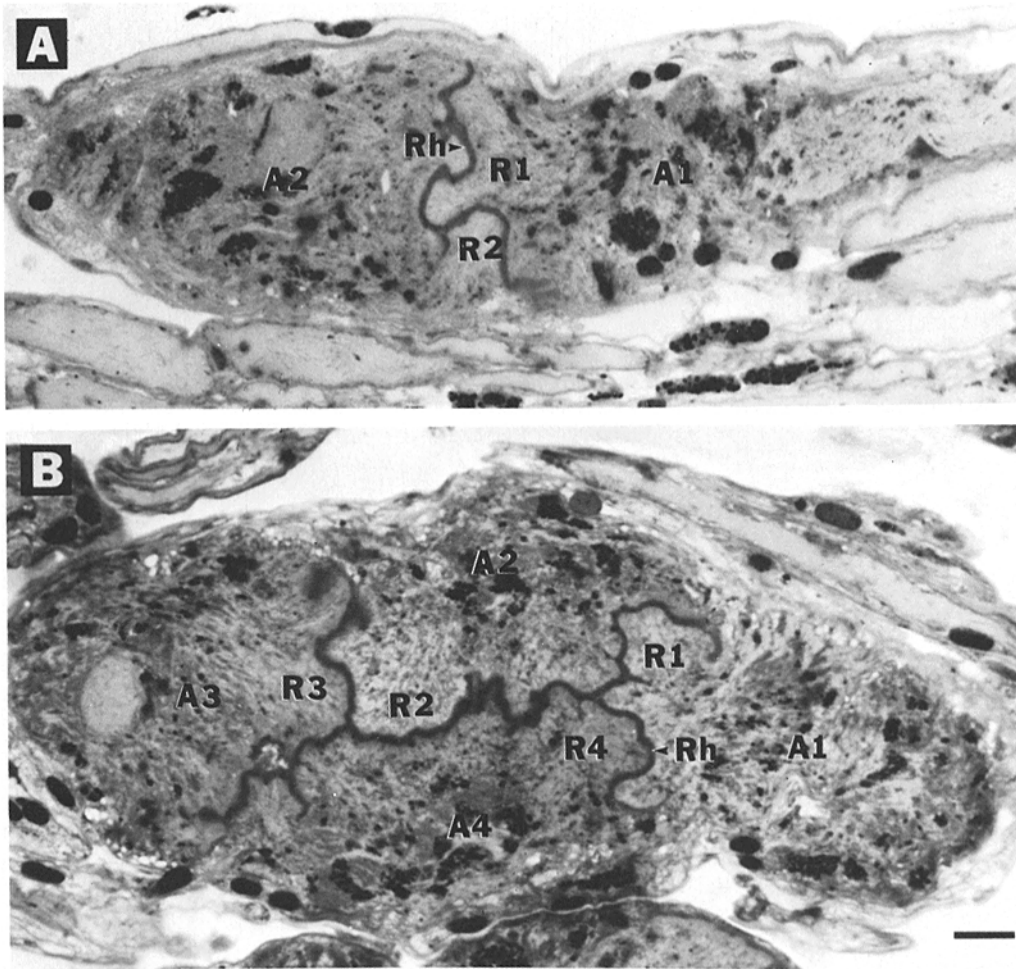

FIGURE 3.   Photomicrographs of clusters of ventral photoreceptors. A. A pair of ventral photoreceptors joined at their R lobes (R1 and R2). B. A cluster of four photoreceptors joined at their R lobes (R1 through R4). In both cases most of the rhabdom (Rh) is internal to the cluster, although external on the individual cells. Reconstructions of the cluster in B are shown in Figs. 6 and 7. A1, A2, A3, A4: A lobes of individual phoreceptors; Rh: rhabdom. The bar in B represents 15 μm in A and 12 μm in B.

Ultrastructure of Ventral Photoreceptors

Figs. 8–12 show electron micrographs of ventral photoreceptors. Clark et al. (1969) outlined the ultrastructural details of these cells rather thoroughly, but did not present their results in the context of the overall segmentation of the
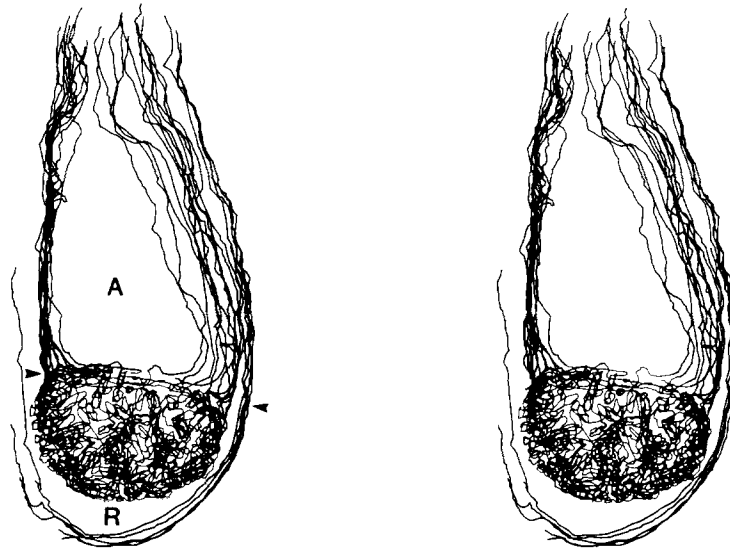
FIGURE 4.   Stereopair computer reconstruction of the single ventral photoreceptor of Fig. 2A. In this and following figures, about half of the computer reconstruction is shown, viewed from the inside. The external surface of the R lobe (R) is completely covered with rhabdom, with several infoldings of rhabdom into the interior. The arrows designate the junction between the R lobe and the A lobe (A). Several profiles of the external boundary of the glial covering are shown.
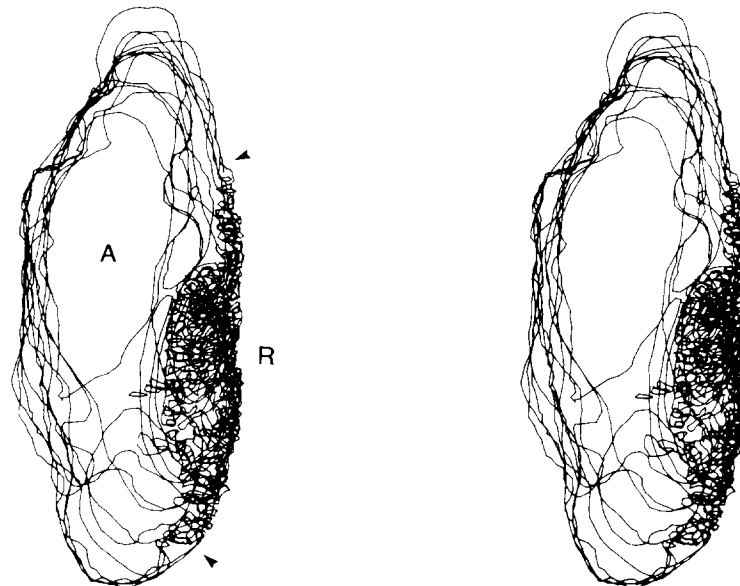

FIGURE 5.   Stereopair computer reconstruction of the single ventral photoreceptor of Fig. 2B. The R lobe (R) occupies a lateral position on this photoreceptor. The arrows designate the junction between the R lobe and the A lobe (A).

photoreceptors. Figs. 8A and 9A show low-magnification micrographs of longitudinal sections near the centers of two different photoreceptors. The cell of Fig. 8A has a structure similar to the cell of Fig. 2A with the R lobe at one end of the cell and the axon at the other. The R lobe of the cell in Fig. 9A occupies both the end and side of the soma. Figs. 8B and D and 9B, D, and

TABLE I

MEASURED VOLUMES AND AREAS OF RHABDOM IN SINGLE VENTRAL PHOTORECEPTORS

Photoreceptor shown in	Total rhabdom	Internal rhabdom	R lobe	Whole cell	Percent internal rhabdom*	Percent R lobe as rhabdom‡	Percent whole cell as rhabdom§	Surface area of rhabdom‖
	μm^3	μm^3	μm^3	μm^3				cm^2
Figs. 2A and 4	6,145.9	986.1	29,939.6	116,006.8	16	20.5	5.3	2.52×10^{-3}
Figs. 2B and 5	5,618.0	1,381.3	42,402.8	133,586.9	24.6	13.2	4.2	2.30×10^{-3}
Fig. 2C	454.2	117.2	1,294.9	7,146.4	25.8	35.1	6.4	1.86×10^{-4}
Fig. 2D								
Left R lobe	1,751.2	278.2	8,758.9		15.9	20		
Right R lobe	2,276.0	566.2	15,706.8		24.9	24.9		
Combined	4,027.2	844.4	24,565.7	115,155.4	21	21.2	3.5	1.65×10^{-3}

* Percent internal rhabdom = (100)(vol internal rhabdom)/(total vol rhabdom).

‡ Percent R lobe as rhabdom = (100)(total vol rhabdom)/(vol R lobe).

§ Percent whole cell as rhabdom = (100)(total vol rhabdom)/(total cell vol).

‖ Surface area calculated from measured microvillar dimensions assuming hexagonal close packing of uniform cylinders; 1 μm^3 of rhabdom volume = 41 μm^2 of rhabdom surface area.
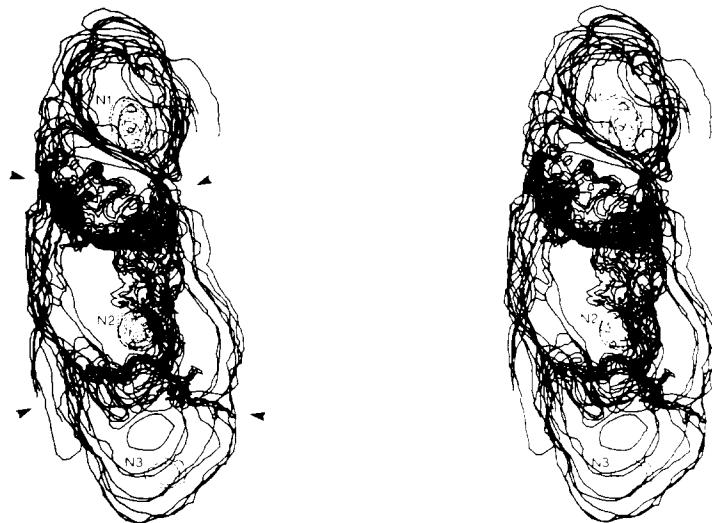

FIGURE 6.   Stereopair computer reconstruction of the four-cell cluster of Fig. 3B. This figure shows half of the total reconstruction, including the nuclei of three of the four cells (N1, N2, N3). The other half is shown in Fig. 7. The arrows indicate the points where the rhabdom reaches the external surface of the cluster. The rhabdom forms a continuous sheet between these points.

E show details of the R lobe. Figs. 8C and E and 9C and F show details of the A lobe. Figs. 10 and 11 show details of the ultrastructure of the rhabdom in single cells and clusters. Fig. 12 shows details of the efferent fibers from the protocerebrum which innervate the photoreceptors.
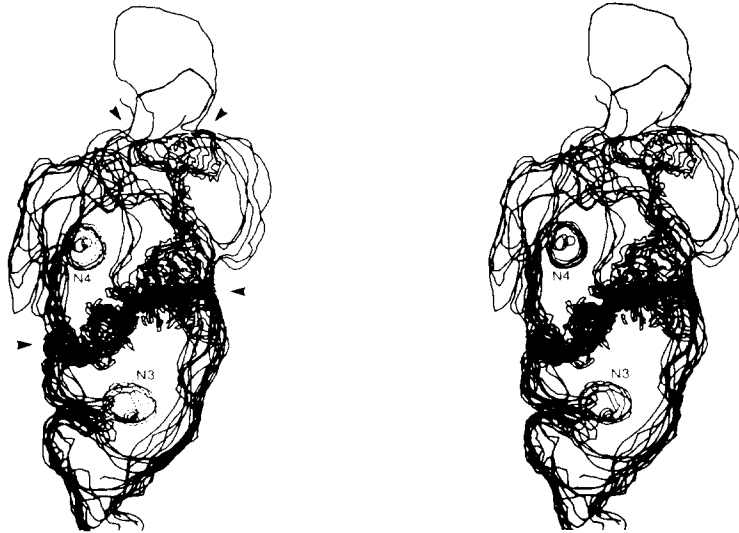

FIGURE 7.   Stereopair computer reconstruction of the other half of the four-cell cluster shown in Fig. 3B. This half includes the nuclei of two of the four cells (N3, N4). The arrows indicate points where the rhabdom reaches the surface of the cluster.

TABLE II

MEASURED VOLUMES AND AREAS OF RHABDOM IN CLUSTERED VENTRAL PHOTORECEPTORS

| Photoreceptor cluster shown in	Number of cells in cluster	Fused external rhabdom	Unfused external rhabdom	Internal rhabdom	Cluster volume	Percent internal rhabdom*	Percent cluster as rhabdom‡	Surface area of rhabdom per cell§
		μm^3	μm^3	μm^3	μm^3			cm^2
Fig. 3A	2	6,164.0	2,571.2	1,492.9	224,598.5	15	4.6	2.10×10^{-3}
Figs. 3B, 6, and 7	4	8,464.6	1,276.0	1,001.3	707,502.0	9.3	3	1.10×10^{-3}

* Percent internal rhabdom = (100)(vol internal rhabdom)/(total vol rhabdom).

‡ Percent cluster as rhabdom = (100)(total vol rhabdom)/(total cluster vol).

§ Surface area calculated from measured microvillar dimensions assuming hexagonal close packing of uniform cylinders; 1 μm^3 of rhabdom volume = 41 μm^2 of rhabdom surface area.

Ultrastructure of the R lobe

The surface of the R lobe is covered by a sheet of microvilli (external rhabdom; Figs. 8A and B and 9A, B, D, and E) joined in some portions of the lobe to invaginations of rhabdom which penetrate inward (internal rhabdom; Figs. 9E and 12A). The external rhabdom is underlain by and the internal rhabdom
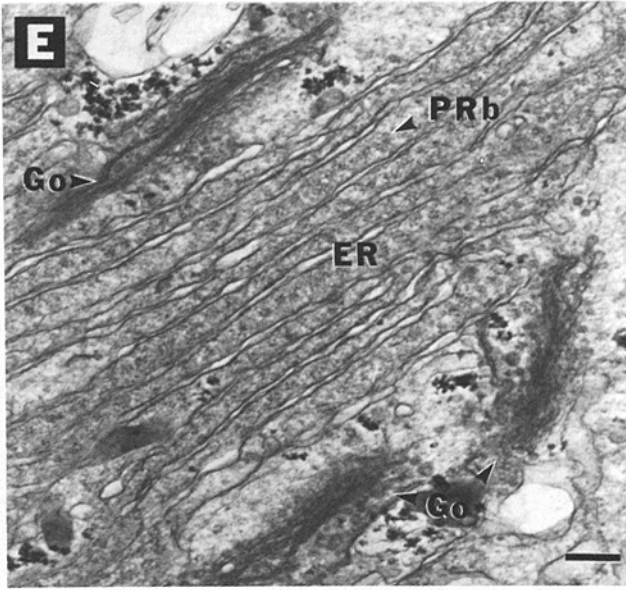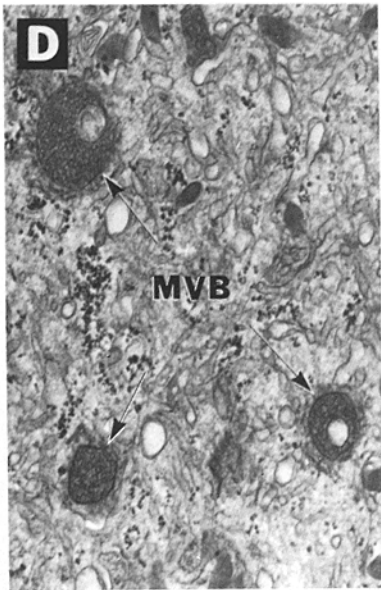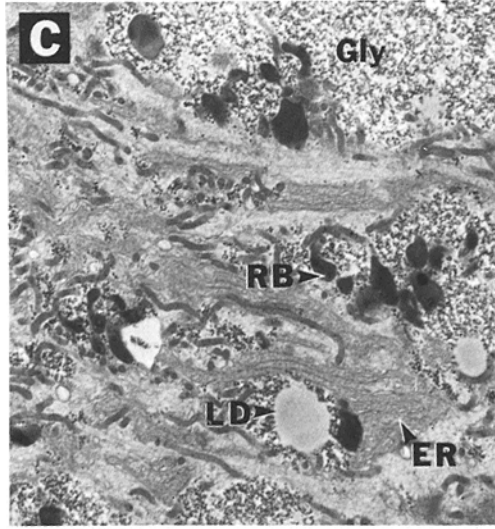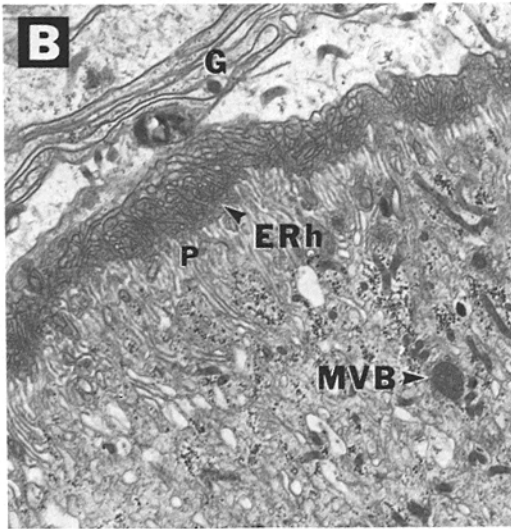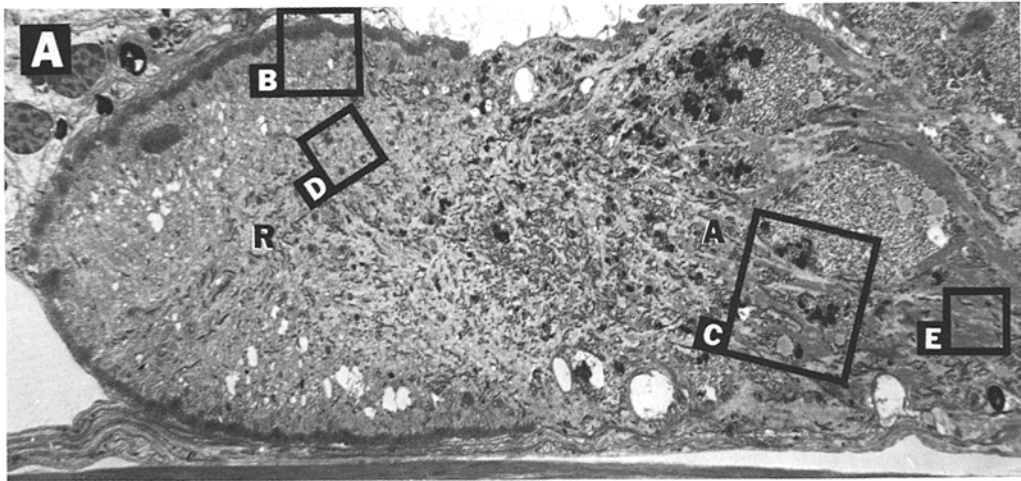
is surrounded by a palisade layer (Figs. 8B and 9B and D; *P*) whose structure resembles the palisade of the lateral eye retinular cells (Fahrenbach, 1969). Under the palisade there is a zone where the organization of the R lobe cytoplasm is striated (Figs. 9A and D). As shown in Fig. 9D, the dark portions contain glycogen and mitochondria whose long axes are oriented parallel to the striations. The light zones contain smooth endoplasmic reticulum and filaments. The light and dark regions are organized in columns perpendicular to the surface of the R lobe. Except for mitochondria and organelles that may be associated with rhabdom turnover (multivesicular bodies, lamellar bodies; Figs. 8B and D), the R lobe is remarkably devoid of other structures.

### Junction between the R Lobe and A Lobe

At the external surface of the photoreceptor, the junction between the two lobes is sharply defined. The external rhabdom covering the R lobe stops (Figs. 9A [arrows] and B) and the surface of the A lobe is smooth. Very often an identation between the two lobes is visible in thin sections and is filled with glial processes (Fig. 9B, *I*). The cytoplasmic boundary between the two lobes is less sharply defined but is characterized by a gradual increase in organelles unique to the A lobe as one moves from the R lobe.

Ultrastructure of the A Lobe

The A lobe contains the nucleus (Fig. 9C) of the photoreceptor and gives rise to the axon. Its cytoplasm has a patchy appearance (Fig. 8C) caused by clumps of residual bodies, lipid droplets, glycogen, endoplasmic reticulum, and mitochondria. The residual bodies (Fig. 8C, *RB*) have the same polymorphic appearance as similar structures in the retinular cells of the lateral eye and are presumed to represent late stages in photoreceptor autophagy, probably of photosensitive membrane. The residual bodies have dark and light areas, regions of lamellar structure, and generally are membrane bound. Lipid droplets (Figs. 8A and C, *LD*) are uniformly circular or elliptical, are not membrane bound, and tend to be associated with clusters of residual

FIGURE 8. (*opposite*) Ultrastructure of single ventral photoreceptor. A. Low-magnification electron micrograph of longitudinal section through whole photoreceptor. The rhabdomeral lobe (R) on the left is completely covered with external rhabdom. The arhabdomeral lobe (A) has mottled cytoplasm. The boxes show approximate areas depicted at higher magnification in B–E. B. Surface of the R lobe. The external rhabdom (ERh) which covers the R lobe abuts glial cells (G) externally and the palisades (P) internally. C. Cytoplasm of the A lobe. Structural features not found in the R lobe include masses of glycogen (Gly), clusters of residual bodies (RB), lipid droplets (LD), and stacks of lamellar endoplasmic reticulum (ER). D. Multivesicular bodies (MVB) in R-lobe cytoplasm. This section is from photoreceptors fixed in mid-morning. E. Higher-magnification electron micrographs of endoplasmic reticulum in the A lobe. The stacks of cisternae have arrays of polyribosomes (PRb) between the lamellae and are often associated with Golgi complexes (Go). The bar in E represents 3.5 μm in A, 0.8 μm in B, 1 μm in C, 0.36 μm in D, and 0.25 μm in E.
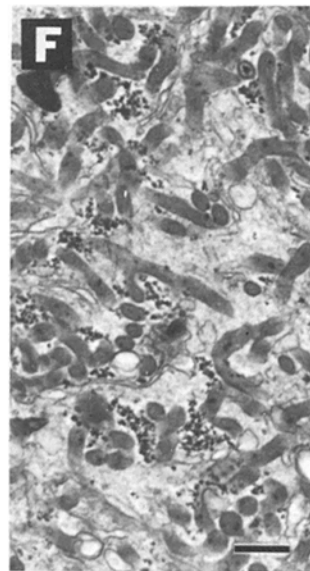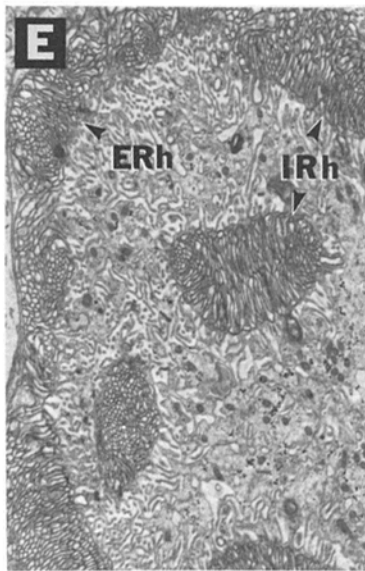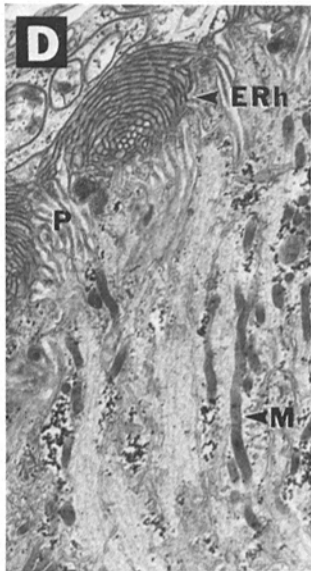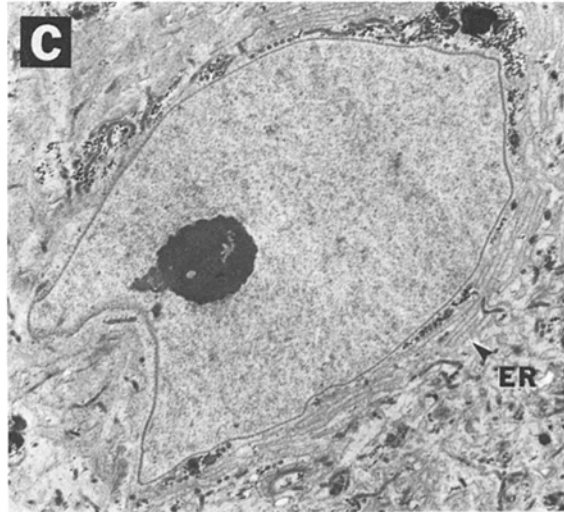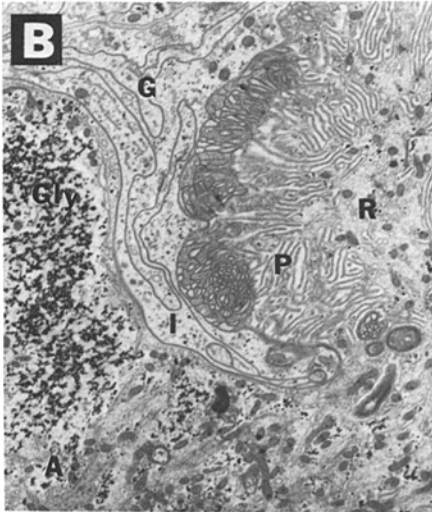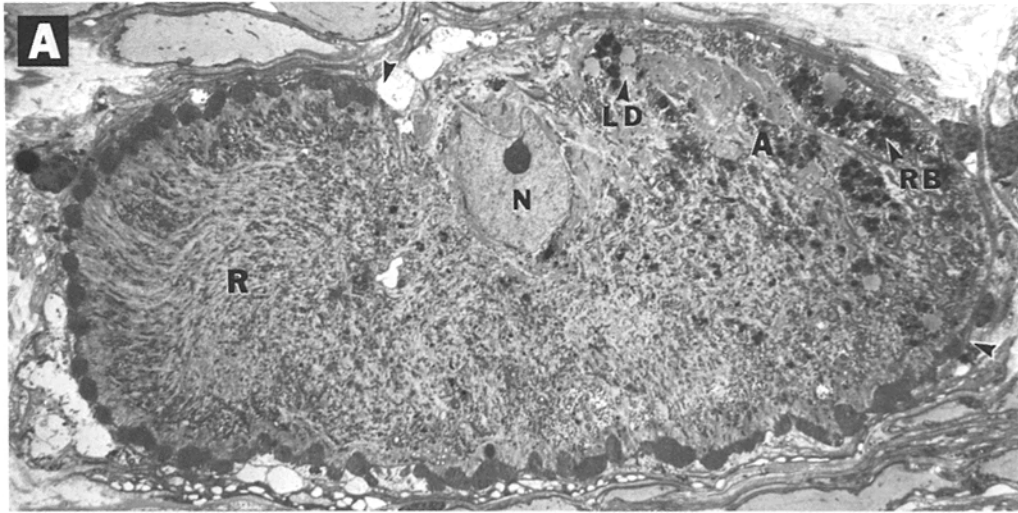
bodies or with large glycogen masses. Glycogen masses (Figs. 8A and C and 9B, *Gly*) as large as 10 μm have been observed. Often the largest accumulations of glycogen are immediately surrounded by lamellar zones of endoplasmic reticulum. Lamellar zones surround the nucleus (Fig. 9C, *ER*) and are distributed throughout the A lobe. The spaces between adjacent sheets of endoplasmic reticulum are filled with arrays of polyribosomes (Fig. 8E, *PRb*), and adjacent regions of cytoplasm often contain associated Golgi complexes (Fig. 8E, *Go*). Clusters of mitochondria (Fig. 9F) contribute to the patchy appearance of the A lobe cytoplasm.

Ultrastructure of the Rhabdom in Single Photoreceptors

Internal rhabdom in the R lobe of single photoreceptors has two different arrangements of microvilli. One arrangement is formed by two abutting layers of microvilli (Fig. 10A), while other internal rhabdom is made up of a single interdigitated layer (Fig. 10B). Both arrangements can occur in the same cell. We have not determined whether all cells possess both types, nor whether there is a compartmentalization of the two types. In our samples, abutting rhabdom was the more common type of internal rhabdom observed.

Definitive generalizations about the structure of the external rhabdom of the R lobe are more problematic. Figs. 10C and D show the appearance of external rhabdom from two cells from the same animal. The rhabdom of adjacent cells may differ greatly in appearance. The differences observed are thus not due to differences in fixation.

Figs. 10C and D show the two appearances of the external rhabdom most frequently seen. Since both are often observed on the surface of the same R lobe, it is possible that they represent two different planes of section through ridges of rhabdom, with Fig. 10C being longitudinal and Fig. 10D being transverse with respect to the long axis of an individual ridge. Alternatively, Fig. 10D might represent a section through a cone of rhabdom. A feature

---

FIGURE 9.   (*opposite*) Ultrastructure of R lobe and A lobe. A. Low-magnification electron micrograph of a longitudinal section through a ventral photoreceptor. The R lobe (R) is covered by external rhabdom (between arrows) and shows the characteristic striations of the cytoplasm perpendicular to the surface. The A lobe (A) contains the nucleus (N), residual bodies (RB), and lipid droplets (LD). B. Junction between R lobe and A lobe. Often an indentation (I) filled with glial processes (G) separates the surface of the R lobe (R) from the A lobe (A). The R lobe contains prominent palisades (P) underlying the external rhabdom. The A lobe shows masses of glycogen (Gly). C. Photoreceptor nucleus in the A lobe. The nucleus may be indented, shows a prominent nucleolus, and is often surrounded by stacks of endoplasmic reticulum (ER). D. Ultrastructure of the R lobe cytoplasm. The striations of the cytoplasm below the external rhabdom (ERh) and palisades (P) are due to dark zones of elongated, oriented mitochondria (M) and glycogen, alternating with light zones showing endoplasmic reticulum and filaments. E. Ultrastructure of the R lobe. Palisades underlie the external rhabdom (ERh) and surround the internal rhabdom (IRh). F. High densities of mitochondria in the A lobe. The bar in F represents 5 μm in A, 1 μm in B, 1.4 μm in C, 0.68 μm in D, 0.91 μm in E, and 0.4 μm in F.

common to these two views is the presence of at least two layers of microvilli. The superficial layer is composed of microvilli whose long axes are parallel to the surface of the R lobe. In Fig. 10C this layer is underlain by a second layer whose microvilli are oriented perpendicular to the surface of the R lobe. In
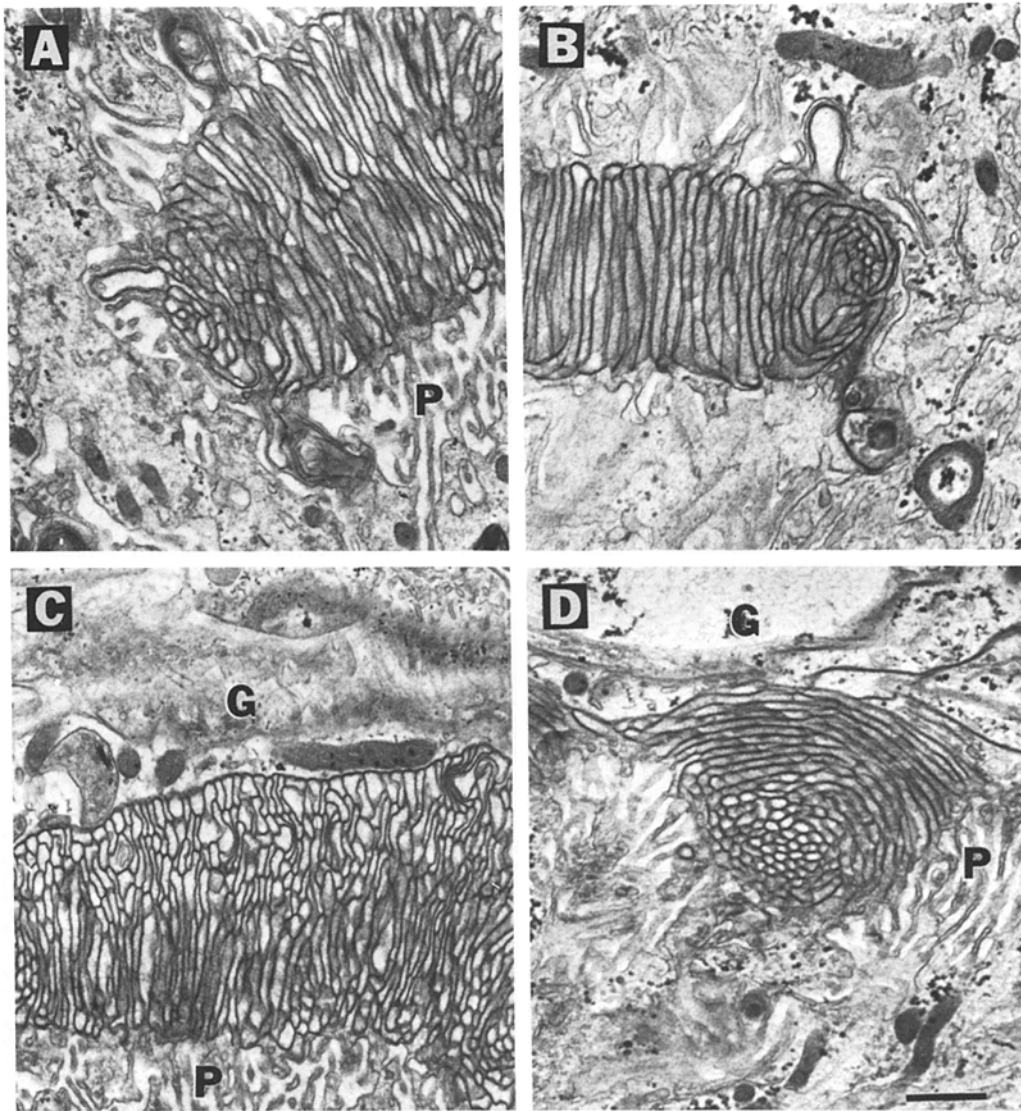
FIGURE 10.   Ultrastructure of the rhabdom in single ventral photoreceptors. A and B show two different arrangements of microvilli in internal rhabdom. Some internal rhabdom has two rows of abutting microvilli A, other internal rhabdom consists of a single row of interdigitated microvilli B. C and D show examples of external rhabdom from photoreceptors from one animal. The rhabdom is composed of several layers of microvilli of differing orientations. G: glial cells; P: palisades. The bar in D represents 0.5 μm.

Fig. 10D there seem to be two mutually perpendicular orientations to the microvilli of the inner layer.

Ultrastructure of the Rhabdom in Clusters of Photoreceptors

Rhabdom in clusters of ventral photoreceptors is essentially of three types. Rhabdom on the surface of the cluster has the same structure as external rhabdom in single photoreceptors (unfused external rhabdom, Table II). Where two R lobes abut in the cluster, the external rhabdom of each contributes to a fused rhabdom made up of two abutting layers of microvilli (fused external rhabdom, Table II). Fig. 11A shows both fused and unfused
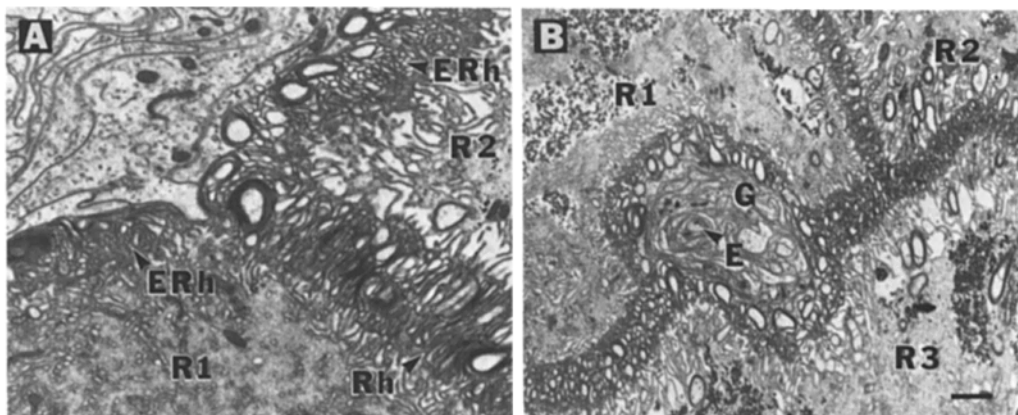

FIGURE 11. Ultrastructure of the rhabdom in clusters of ventral photoreceptors. A. External rhabdom (ERh) in individual cells of the cluster has the same structure as in single cells when it faces glial processes (upper left corner), but forms half of a double thickness of abutting microvilli (Rh) when the rhabdom is internal to the cluster between two cells (R1, R2). B. Rhabdom internal to a cluster of ventral photoreceptors is formed by abutting external rhabdom of R lobes of three different photoreceptors (R1, R2, R3). The two abutting layers of microvilli are interrupted by a glial invagination (G), which contains at least one identifiable efferent fiber (E). The bar in B represents 0.63 μm in A and 1.19 μm in B.

external rhabdom at a point where abutted rhabdom, internal to the cluster, reaches the cluster's surface and becomes unfused external rhabdom. The third type of rhabdom is also of the double-layered abutting type and is found internal to individual cells of the cluster, formed as invaginations from either type of external rhabdom (internal rhabdom, Table II). Figs. 11A and B show fused external rhabdom, and Fig. 12A shows internal rhabdom.

Ultrastructure of Other Elements: Glia and Efferent Fibers

Ventral photoreceptors, singly and in clusters, are ensheathed in layers of glial cells. We have observed breaks in the glial cover over both R and A lobes, but such zones of direct contact between the photoreceptor membrane and the hemolymph appear to be rare. Fingers of glia occasionally penetrate the

somata of single photoreceptors, protruding into the R lobe. The indentation between the R lobe and A lobe is also filled with glial processes. We have not observed significant glial invaginations into the A lobe except at or near the indentation at the boundary with the R lobe. In clusters, glial fingers are common within the rhabdom internal to the cluster (Fig. 11B, G).

Efferent fibers that innervate the photoreceptors from the protocerebrum enter the R lobe of single cells and the rhabdom of clusters in these glial fingers. The results of studies of efferent morphology using labeled efferents and autoradiography have been reported separately (Battelle and Chamberlain, 1980; Battelle et al., 1982; Evans et at., 1982). Our examination of normal tissue revealed that efferent fibers have relatively lucent cytoplasm, and contain mitochondria, filaments, and two types of vesicles—small, lucent circular profiles (Fig. 12B), and large, darkly staining, angular granules (Fig. 12A, white arrow). Contacts between the efferents and photoreceptors probably involve the same type of synaptoid specialization found in the lateral eye (Fahrenbach, 1973; Barlow and Chamberlain, 1980; Fahrenbach, 1981). Although we have not observed synapses directly, several sections show concentration of clear vesicles close to well-apposed membranes which suggest that the section was close to a synaptoid specialization (Fig. 12B). In single photoreceptors, efferent profiles appear within the glial sheath, but separated from the photoreceptor itself; immediately apposed to the R lobe membrane just at the end of the external rhabdom (Fig. 12B); and in glial invaginations associated with internal rhabdom. Very often efferent fibers are immediately apposed to the microvilli of the internal rhabdom without interposed glial profiles (Fig. 12A). In clusters, efferents are found within glial fingers associated with the rhabdom within the cluster (Fig. 11B) and directly apposed to the abutting rhabdom itself (Fig. 12A). We have not observed efferent fibers in the A lobe. If we take direct apposition between efferent fibers and other structures as indicative of a presynaptic–postsynaptic relationship, we conclude that the rhabdom of the R lobes of single cells and cell clusters is the primary, if not exclusive, target of efferent fibers.

DISCUSSION

Segmentation of Ventral Photoreceptors

The ventral photoreceptors of *Limulus* are divided into lobes that appear to be morphologically and physiologically specialized. One type, the R lobe, contains all the rhabdom. Several types of evidence in other systems, including microspectrophotometry (Langer and Thorell, 1966), freeze-fracture (Nickel and Menzel, 1976; Fernandez and Nickel, 1976; Eguchi and Waterman, 1976), and electrophysiology of the developing eye (Eguchi et al., 1962) indicate that the rhabdom contains the photosensitive pigment in invertebrates. The R lobe also contains the organelles, which are shown in the lateral eye (Chamberlain and Barlow, 1979) to be part of the rhabdom breakdown process. When denuded of its glial covering, the R lobe is still at least 100

times more sensitive to light than the remainder of the photoreceptor (Stern et al., 1982). The R lobe thus seems to be the area of cell specialized for photon absorption analogous to the outer segment of vertebrate photoreceptors.

The other type of lobe, the A lobe, contains high densities of all the organelles necessary for metabolism. The presence of large arrays of endoplas-
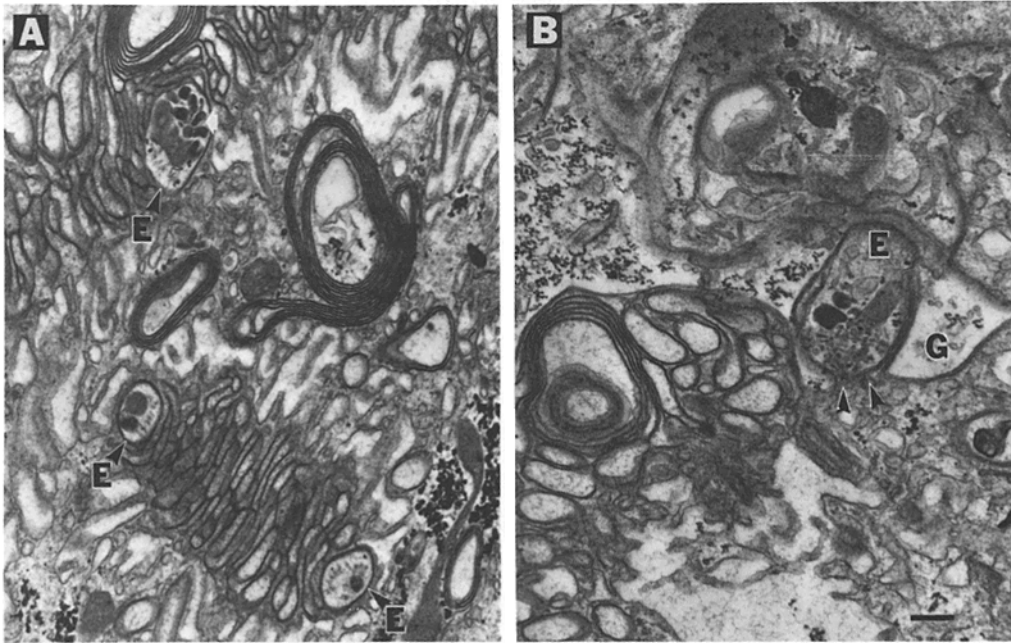
FIGURE 12.   Efferent innervation of ventral photoreceptors. A. Efferent profiles contacting fused external (upper) and internal rhabdom (lower) of a cell in a cluster. The white arrow indicates characteristic dense granules in efferent profiles. All these profiles are immediately apposed to rhabdom without intervening glial processes. B. Synaptoid specialization (dark arrows) between an efferent fiber (E) and a ventral photoreceptor at the junction between the R lobe and A lobe. The efferent profile contains both dark granules and smaller lucent vesicles. Synaptoid specializations occur at interruptions in the glial investment (G) of the efferent fibers. The bar in B represents 0.27 μm in A and 0.24 μm in B.

mic reticulum and Golgi complexes and regions dense with mitochondria suggests that the A lobe is active in energy transport and macromolecule synthesis. These functions are analogous to those of vertebrate photoreceptor inner segments.

The segmentation of ventral photoreceptors was not reported in the earlier study of Clark et al. (1969). We suggest that they did not observe the

segmentation for two reasons. First, their micrographs suggest that their procedure did not preserve most of the external rhabdom. Second, without careful observations of serial sections, it is easy to mistake clusters of small numbers of cells for single cells. Both of these problems may have contributed to the production of their summary drawing of the structure of a single cell, which showed only a hint of external rhabdom, and placed the internal rhabdom between the nucleus and the axon, an arrangement we have never observed.

Structure of the Rhabdom

From light microscopy and computer reconstructions we have concluded that the rhabdom of a single R lobe is equivalent to a single sheet. Our examination of the ultrastructure of the external rhabdom, however, has failed to answer two potentially important questions. Although we noted in some cells indications of a substructure in the gross arrangement of the external rhabdom over the surface of the R lobe, we have no strong evidence about what the normal arrangement is nor how much variability there might be. We have also been unable to determine the detailed arrangement of the microvilli within the external rhabdom. Observations of our best-organized external rhabdom suggests that the ultrastructure of this organelle may be interesting and complex, involving several layers of microvilli in three-dimensional arrays with different microvillar orientations.

The central difficulty in our determining the ultrastructure of the external rhabdom was the variability of its appearance from one photoreceptor to another. The full range of variability seen from one animal to another was also observable from cell to cell in a single animal. The source of this variability has not been established. Perhaps our fixation procedure is not yet adequate to preserve the external rhabdom. It might also be that in mid-morning (the time of fixation), the rhabdom is in the midst of membrane turnover, causing cell-to-cell variation in rhabdom ultrastructure. Other lines of evidence, however, suggest that external rhabdom may be particularly sensitive to the adversities of dissection, incubation, and fixation in vitro. Clark et al. (1969) used essentially the same fixation procedure we used, except that the photoreceptors were dissected from the animals and fixed in vitro. Their micrographs showed excellent preservation of the ultrastructure, but little or no external rhabdom. Likewise, Battelle et al. (1982) incubated ventral photoreceptors overnight before fixing them in vitro for ultrastructural study. Their micrographs show excellent preservation of the internal rhabdom, but essentially no external rhabdom. Stern et al. (1982) observed lobes in all cells fixed in vitro but found external microvilli covering the R lobe in a fraction of the cells examined. The appearance of the microvilli on the surface of the R lobe was different from that which we observed in cells fixed in vivo. We conclude that all ventral photoreceptor R lobes normally possess extensive external rhabdom which can be observed consistently if the cells are fixed in vivo. The suggestion that the external rhabdom may disappear or undergo massive changes under some conditions of dissection and incubation casts in

a new light the findings of Bayer and Barlow (1978). They found that using organ culture or low temperatures for incubating photoreceptors in vitro changed their physiological properties and extended their viability. The ultrastructure of ventral photoreceptors in various physiological protocols merits further study.

FIGURE 13. Summary drawing of a single *Limulus* ventral photoreceptor showing the two lobes and distribution of important structures. Some simplifications have been made in the drawing (see text). E: efferent fiber; ER: endoplasmic reticulum; ERh: external rhabdom; G: glial cells; Gly: glycogen; Go: Golgi complex; GN: nucleus of glial cell; I: glia-filled indentation at junction of R lobe and A lobe; IRh: internal rhabdom; LD: lipid droplet; M: mitochondria; MVB: multivesicular body; N: nucleus; P: palisade; RB: residual body.

Efferent Innervation of the R Lobe

Efferent fibers in the *Limulus* lateral eye have been implicated in a wide variety of phenomena, including control of rhabdom turnover (Chamberlain and Barlow, 1979), suppression of spontaneous large and small potential fluctuations in dark-adapted retinular cells (Kaplan and Barlow, 1980), modulation of photoreceptor sensitivity (Barlow et al., 1977) and acceptance angle (Barlow et al., 1980), and control of photomechanical movements (Chamberlain and Barlow, 1981). In the lateral eye, efferent fibers make contact with all cell types (Fahrenbach, 1981). Since our results and those of

Evans et al. (1982) suggest that the rhabdom itself is the primary target of the efferent fibers to the ventral eye, it would seem that the control of rhabdom turnover and suppression of spontaneous potential fluctuations might be two processes under efferent control in this photoreceptor. Neither rhabdom turnover nor its control mechanisms have been studied in ventral photoreceptors. Likewise, no one has yet been able to demonstrate efferent suppression of spontaneous potential fluctuations in dark-adapted ventral photoreceptors. The central thrust of our study and that of Stern et al. (1982), coupled with the findings of Battelle et al. (1982) that efferent fibers in the ventral eye synthesize and release octopamine, suggest that this preparation may be very useful for the study of efferent function and basic phototransduction, in a system simpler than the lateral eye, but one that is still structurally and functionally well organized.

Summary of Ventral Photoreceptor Structure

Fig. 13 shows a cutaway sketch of the structure of a single ventral photoreceptor. The drawing has been simplified in a number of ways for clarity, including the representation of the external rhabdom as a single layer of microvilli, and the cristae of the mitochondria as transverse rather than the more commonly observed longitudinal. Not all the organelles are shown to scale.

This drawing emphasizes the segmentation of the ventral photoreceptor into a rhabdomeral lobe which contains, as its principal organelle, the rhabdomere; and an arhabdomeral lobe which seems to contain much of the cell's cytoplasmic machinery. Since the rhabdomere contains the photosensitive pigment in invertebrate photoreceptors, the R lobe would indeed appear to be a specialized segment of ventral photoreceptors for photon absorption, as evidenced by its much greater sensitivity to light (Stern et al., 1982).

REFERENCES

Bacigalupo, J., J. Stern, and J. Lisman. 1981. Structural and functional specialization of *Limulus* ventral photoreceptor membrane. *Invest. Ophthalmol. Vis. Sci.* **20**(Suppl.):181. (Abstr.).

Barlow, R. B., Jr., S. J. Bolanowski, Jr., and M. L. Brachman. 1977. Efferent optic nerve fibers mediate circadian rhythms in the *Limulus* eye. *Science* (*Wash. D. C.*). **197**:86–89.

Barlow, R. B., Jr., and S. C. Chamberlain. 1980. Light and a circadian clock modulate structure and function in *Limulus* photoreceptors. *In* The Effects of Constant Light on Visual Processes. T. P. Williams and B. N. Baker, editors. Plenum Press, New York. 247–269.

BARLOW, R. B., JR., S. C. CHAMBERLAIN, and J. Z. LEVINSON. 1980. *Limulus* brain modulates the structure and function of the lateral eye. *Science (Wash. D. C.).* **210:**1037–1039.

BATRA, R., M. BEHRENS, and S. CHAMBERLAIN. 1979. *Limulus* ventral photoreceptors: do they send information to the brain? *Soc. Neurosci. Abstr.* **5:**776.

BATTELLE, B. A., and S. C. CHAMBERLAIN. 1980. Autoradiographic localization of sites of octopamine synthesis in *Limulus* ventral eye. *Soc. Neurosci. Abstr.* **6:**702.

BATTELLE, B. A., J. A. EVANS, and S. C. CHAMBERLAIN. 1982. Efferent fibers to *Limulus* eyes synthesize and release octopamine. *Science (Wash. D. C.).* **216:**1250–1252.

BATTELLE, B. A., E. A. KRAVITZ, and H. STIEVE. 1979. Neurotransmitter synthesis in *Limulus* ventral nerve photoreceptors. *Experientia.* **35:**778–780.

BAYER, D. S., and R. B. BARLOW, JR. 1978. *Limulus* ventral eye. Physiological properties of photoreceptor cells in an organ culture medium. *J. Gen. Physiol.* **72:**539–563.

BEHRENS, M. E., and J. L. FAHEY. 1981. Slow potentials in nonspiking optic nerve fibers in the peripheral visual system of *Limulus. J. Comp. Physiol.* **141:**239–247.

CHAMBERLAIN, S. C. 1978. Neuroanatomy of the visual afferents in *Limulus polyphemus.* Doctoral Dissertation and Institute for Sensory Research Special Report LSC-16, Syracuse University, Syracuse, NY.

CHAMBERLAIN, S. C., and R. B. BARLOW, JR. 1979. Light and efferent activity control rhabdom turnover in *Limulus* photoreceptors. *Science (Wash. D. C.).* **206:**361–363.

CHAMBERLAIN, S. C., and R. B. BARLOW, JR. 1981. Modulation of retinal structure in *Limulus* lateral eye; interactions of light and efferent inputs. *Invest. Ophthalmol. Vis. Sci.* **20**(Suppl.):75. (Abstr.).

CLARK, A. W., R. MILLECCHIA, and A. MAURO. 1969. The ventral photoreceptor cells of *Limulus.* I. The microanatomy. *J. Gen. Physiol.* **54:**289–309.

EGUCHI, E., K. NAKA, and M. KUWABARA. 1962. The development of the rhabdom and the appearance of the electrical response in the insect eye. *J. Gen. Physiol.* **46:**143–157.

EGUCHI, H., and T. H. WATERMAN. 1976. Freeze-etch and histochemical evidence for cycling in crayfish photoreceptor membranes. *Cell Tissue Res.* **169:**419–434.

EVANS, J. A., S. C. CHAMBERLAIN, and B. A. BATTELLE. 1982. Efferent fibers to *Limulus* eyes synthesize and store octopamine. *J. Comp. Neurol.* In press.

FAHRENBACH, W. H. 1969. The morphology of the eyes of *Limulus.* II. Ommatidia of the compound eye. *Z. Zellforsch.* **93:**451–483.

FAHRENBACH, W. H. 1970. The morphology of the *Limulus* visual system. III. The lateral rudimentary eye. *Z. Zellforsch.* **105:**303–316.

FAHRENBACH, W. H. 1973. The morphology of the *Limulus* visual system. V. Protocerebral neurosecretion and ocular innervation. *Z. Zellforsch.* **144:**153–166.

FAHRENBACH, W. H. 1981. The morphology of the horseshoe crab (*Limulus polyphemus*) visual system. VII. Innervation of photoreceptor neurons by neurosecretory efferents. *Cell Tissue Res.* **216:**655–659.

FAIN, G. L., and J. E. LISMAN. 1981. Membrane conductances of photoreceptors. *Prog. Biophys. Mol. Biol.* **37:**91–147.

FERNANDEZ, H. R., and E. E. NICKEL. 1976. Ultrastructural and molecular characteristics of crayfish photoreceptor membranes. *J. Cell Biol.* **69:**721–732.

HANSTRÖM, B. 1926. Das Nervensystem und die Sinnesorgane von *Limulus polyphemus. Lunds Univ. Arsskrift.* N.F. Avd. 2, Bd. 22, Nr. 5:1–78.

KAPLAN, E., and R. B. BARLOW, JR. 1980. Circadian clock in *Limulus* brain increases response and decreases noise of retinal photoreceptors. *Nature (Lond.).* **286:**393–395.

LANGER, H., and B. THORELL. 1966. Microspectrophotometry of single rhabdomeres in the insect eye. *Exp. Cell Res.* **41:**673-677.

MILLECCHIA, R., J. BRADBURY, and A. MAURO. 1966. Simple photoreceptors in *Limulus polyphemus. Science (Wash. D. C.).* **154:**1199-1201.

MILLECCHIA, R., and A. MAURO. 1969a. The ventral photoreceptor cells of *Limulus.* II. The basic photoresponse. *J. Gen. Physiol.* **54:**310-330.

MILLECCHIA, R., and A. MAURO. 1969b. The ventral photoreceptor cells of *Limulus.* III. A voltage-clamp study. *J. Gen. Physiol.* **54:**331-351.

NICKEL, E., and R. MENZEL. 1976. Insect UV- and green-photoreceptor membranes studied by the freeze-fracture technique. *Cell Tissue Res.* **175:**357-368.

PATTEN, W. 1893. On the morphology and physiology of the brain and sense organs of *Limulus. Q. J. Micro. Sci.* **35:**1-96.

PATTEN, W. 1912. The Evolution of the Vertebrates and Their Kin. Blakiston, Philadelphia, PA. 481 pp.

SNODDERLY, D. M., JR. 1971. Processing of visual inputs by brain of *Limulus. J. Neurophysiol.* **34:**588-611.

STELL, W. H., and M. J. RAVITZ. 1970. The structure of neurons in the ventral photoreceptor organ of the horseshoe crab *Limulus polyphemus. J. Cell Biol.* **47:**202a. (Abstr.).

STERN, J., K. CHINN, J. BACIGALUPO, and J. LISMAN. 1982. Distinct lobes of *Limulus* ventral photoreceptors. I. Functional and anatomical properties of lobes revealed by removal of glial cells. *J. Gen. Physiol.* **80:**825-837.

TRUMP, B. F., E. A. SMUCKLER, and E. P. BENDITT. 1961. A method for staining epoxy sections for light microscopy. *J. Ultrastruct. Res.* **5:**343.

WASSERMAN, G. S. 1973. Unconditioned response to light in *Limulus:* mediation by lateral, median, and ventral eye loci. *Vis. Res.* **13:**95-105.